ADVANCES IN ATMOSPHERIC SCIENCES, VOL. 20, NO. 5, 2003, PP. 825–836

# Up-Sliding Slantwise Vorticity Development and the Complete Vorticity Equation with Mass Forcing

CUI Xiaopeng* (崔晓鹏), GAO Shouting (高守亭), and WU Guoxiong (吴国雄)

*Institute of Atmospheric Physics, Chinese Academy of Sciences, Beijing* 100029

(Received 14 August 2002; revised 19 June 2003)

**ABSTRACT**

The moist potential vorticity (MPV) equation is derived from complete atmospheric equations including the effect of mass forcing, with which the theory of Up-sliding Slantwise Vorticity Development (USVD) is proposed based on the theory of Slantwise Vorticity Development (SVD). When an air parcel slides up along a slantwise isentropic surface, its vertical component of relative vorticity will develop, and the steeper the isentropic surface is, the more violent the development will be. From the definition of MPV and the MPV equation produced here in, a complete vorticity equation is then put forward with mass forcing, which explicitly includes the effects of both internal forcings, such as variations of stability, baroclinicity, and vertical shear of horizontal wind, and external forcings, such as diabatic heating, friction, and mass forcing. When isentropic surfaces are flat, the complete vorticity equation matches its traditional counterpart. The physical interpretations of some of the items which are included in the complete vorticity equation but not in the traditional one are studied with a simplified model of the Changjiang-Huaihe Meiyu front. A 60-h simulation is then performed to reproduce a torrential rain event in the Changjiang-Huaihe region and the output of the model is studied qualitatively based on the theory of USVD. The result shows that the conditions of the theory of USVD are easily satisfied immediately in front of mesoscale rainstorms in the downwind direction, that is, the theory of USVD is important to the development and movement of these kinds of systems.

**Key words:** Up-sliding Slantwise Vorticity Development (USVD), mass forcing, complete vorticity equation

## 1. Introduction

The concept of potential vorticity (defined as $(\boldsymbol{\zeta}_{\mathrm{a}} \cdot \nabla\theta)/\rho$, hereafter referred to as Ertel PV), first introduced by Ertel (1942), is fundamental to our understanding of atmospheric dynamics. In a frictionless and adiabatic dry atmosphere, Ertel PV is conserved. Besides its conservation, Ertel PV also has two other main properties: its invertibility in a balanced system and the impermeability of PV substance. Ertel PV is very useful in both diagnostic and prognostic studies of atmospheric phenomena (Robinson, 1989; Gao et al., 1990; Hoskins and Berrisford, 1988; Davis and Emanuel, 1991; Schubert and Alworth, 1987; Thorpe, 1990; Montgomery and Farrell, 1992; Keyser and Rotunno, 1990). Pedlosky (1979) stressed that the PV notion is so important that the emphasis on it can never be overdone. The application of Ertel PV in the diagnosis of atmospheric motion was summarized by Hoskins et al. (1985), and the concept of isentropic potential vorticity (IPV) was also introduced. IPV is indicative of some aspects of the movement and development of weather systems in middle and high latitudes. But in the lower troposphere, especially in low latitudes, IPV has some limitations.

When moisture is too important to be neglected, such as in the study of torrential rains, the definition and concept of PV are also available except that now $\theta$ (potential temperature) is replaced by $\theta_{\mathrm{e}}$ (equivalent potential temperature) in the expression of PV, and since the effect of moisture is involved, the new PV is called moist potential vorticity (MPV). Bennetts and Hoskins (1979) deduced an equation for the variation of the so-called “wet-bulb potential vorticity” by using a set of equations with the Boussinesq approximation and concluded that conditional symmetric instability is a possible cause of formation of frontal rain belts. Based on the precise primitive equations, a similar

*E-mail: xpcui@mail.iap.ac.cn

variation equation for MPV was also obtained by Wu et al. (1998, 1995, 1997, 1999), which shows that in a frictionless and adiabatic saturated atmosphere, MPV is conserved, and the theory of Slantwise Vorticity Development (SVD) was proposed to study the development of the vertical component of relative vorticity in a moist baroclinic condition; according to the theory, vorticities are apt to develop near steep isentropic surfaces. In fact, since many kinds of weather systems in the atmosphere do occur and develop near slantwise (moist) isentropic surfaces, it is applicable and necessary to investigate the evolution of these systems in the context of slantwise isentropic surfaces. A new form of vertical vorticity equation was also produced by Wu et al. (1999) based on the definition of PV and MPV. Compared to the traditional vertical vorticity equation, the new one has many advantages and is more applicable for diagnosis (Wu, 2001). To study torrential rains, an MPV equation was also derived by Gao et al. (2002) with mass forcing and the impermeability of the MPV substance was proved. They concluded that the MPV substance anomaly induced by both heating and mass forcing during torrential rains is a good tracer for tracking the region of torrential rains, which can be useful in the forecast of torrential rains.

Some studies (Zhang et al., 1999; Cui, 2001) showed that up-sliding slantwise movements are always observed during the development and movement of oceanic frontal cyclones and rainstorms in the Changjiang-Huaihe valley, which prompts us to improve the theory of SVD to make it suitable for this situation. In this article, at first an MPV equation is derived with diabatic heating, friction, and mass forcing in section 2, and then the theory of up-sliding slantwise vorticity development (USVD) is proposed in section 3. Furthermore, a complete vorticity equation is produced in section 4. By comparing the complete vorticity equation with the traditional one, some items not included in the latter are obtained, and by taking the simplified Changjiang-Huaihe Meiyu front as an example, the physical interpretations of these items are analyzed in section 5. In section 6, a 60-h simulation of a torrential rain event in the Changjiang-Huaihe region is analyzed qualitatively based on the theory of USVD. Conclusions and discussion are given in section 7.

## 2. Moist potential vorticity equation with mass forcing

By taking the vector product of the momentum equation, and being aware of the fact that the vector product of a gradient is zero, we obtain the vorticity equation

$$\frac{\partial \boldsymbol{\zeta}_{\mathrm{a}}}{\partial t} - \nabla \times (\boldsymbol{V} \times \boldsymbol{\zeta}_{\mathrm{a}}) = \nabla p \times \nabla \alpha + \nabla \times \boldsymbol{F} \; , \quad (2.1)$$

where

$$\boldsymbol{\zeta}_{\mathrm{a}} = \nabla \times \boldsymbol{V} + 2\boldsymbol{\Omega}$$

is the absolute vorticity.

$$\alpha = \frac{1}{\rho} \; ,$$

and $\rho$ is the air density.

Including latent heating and other kinds of heating $Q_{\mathrm{d}}$, the thermodynamic equation can be written as

$$c_p \frac{T}{\theta}\frac{d\theta}{dt} = -L\frac{dq}{dt} + Q_{\mathrm{d}} \; . \quad (2.2)$$

Upon taking the natural logarithm and total derivative of both sides of the definition of equivalent potential temperature

$$\theta_{\mathrm{e}} = \theta \exp\left(\frac{Lq}{c_p T}\right) \; ,$$

putting it into the above thermodynamic equation, (2.2), and omitting the high-order term, we obtain

$$\frac{d\theta_{\mathrm{e}}}{dt} = \frac{\theta_e}{c_p T} Q_{\mathrm{d}} = Q \; . \quad (2.3)$$

By taking the scalar product of (2.1) with $\nabla\theta_{\mathrm{e}}$, we obtain

$$\alpha \frac{d(\boldsymbol{\zeta}_{\mathrm{a}} \cdot \nabla\theta_{\mathrm{e}})}{dt} = -\alpha(\boldsymbol{\zeta}_{\mathrm{a}} \cdot \nabla\theta_{\mathrm{e}})\nabla \cdot \boldsymbol{V}$$
$$+ \alpha(\nabla p \times \nabla\alpha) \cdot \nabla\theta_{\mathrm{e}} + \alpha\boldsymbol{\zeta}_{\mathrm{a}} \cdot \nabla Q + \alpha\nabla\theta_{\mathrm{e}} \cdot (\nabla \times \boldsymbol{F}) \; . \quad (2.4)$$

When it is raining, the continuity equation can be expressed as (referring to Gao et al., 2002)

$$\frac{d\rho_{\mathrm{a}}}{dt} + \rho_{\mathrm{a}} \nabla \cdot \boldsymbol{V} = -\nabla \cdot (\rho_{\mathrm{r}} \boldsymbol{V}_t) \; , \quad (2.5)$$

where $\boldsymbol{V}_t$ is the terminal velocity of a precipitation particle and

$$-\nabla \cdot (\rho_{\mathrm{r}} \boldsymbol{V}_t)$$

is the contribution of mass forcing caused by precipitation to the variation of density;

$$\rho_{\mathrm{a}} = \rho_{\mathrm{d}} + \rho_{\mathrm{v}} + \rho_{\mathrm{c}} + \rho_{\mathrm{r}}$$

with $\rho_{\mathrm{a}}$ being the general density, and $\rho_{\mathrm{d}}, \rho_{\mathrm{v}}, \rho_{\mathrm{c}}$, and $\rho_{\mathrm{r}}$ the densities of dry air, vapor, cloud water, and rain water, respectively. There exist the following continuity equations

$$\frac{d\rho_{\mathrm{d}}}{dt} + \rho_{\mathrm{d}} \nabla \cdot \boldsymbol{V} = 0 \; , \quad (2.6)$$

$$\frac{d\rho_{\mathrm{v}}}{dt} + \rho_{\mathrm{v}} \nabla \cdot \boldsymbol{V} = -Q_{\mathrm{v}} \; , \quad (2.7)$$

$$\frac{d\rho_{\mathrm{w}}}{dt} + \rho_{\mathrm{w}} \nabla \cdot \boldsymbol{V} + \nabla(\rho_{\mathrm{r}} \boldsymbol{V}_t) = Q_{\mathrm{v}} \; , \quad (2.8)$$

where

$$\rho_{\rm w}=\rho_{\rm c}+\rho_{\rm r}\ ,$$

and $Q_{\rm v}$ is the transfer function from vapor to cloud water and rain water; Then the air continuity equation is obtained by substituting (2.7) into (2.6), namely

$$\frac{d\alpha}{dt}=\alpha\nabla\cdot\boldsymbol{V}+\alpha^2Q_{\rm v}=\alpha\nabla\cdot\boldsymbol{V}+Q_{\rm n}\ , \qquad (2.9)$$

where

$$\alpha=\frac{1}{\rho},\ \rho=\rho_{\rm d}+\rho_{\rm v}\ ,$$

and

$$Q_{\rm n}=\alpha^2Q_{\rm v}$$

is the contribution of mass forcing caused by precipitation and condensation to the variation of density.

By multiplying

$$\boldsymbol{\zeta}_{\rm a}\cdot\nabla\theta_{\rm e}$$

on both sides of (2.9), and substituting it into (2.4), defining

$$\boldsymbol{F}_\xi=\nabla\times\boldsymbol{F}$$

as the eddy friction diffusion and

$$P_{\rm m}=\alpha\boldsymbol{\zeta}_{\rm a}\cdot\nabla\theta_{\rm e}$$

as MPV, the MPV equation with mass forcing is found to be

$$\begin{aligned}\frac{dP_{\rm m}}{dt}&=\alpha(\nabla p\times\nabla\alpha)\cdot\nabla\theta_{\rm e}+\alpha\boldsymbol{\zeta}_{\rm a}\cdot\nabla Q\\&+\alpha\nabla\theta_{\rm e}\cdot\boldsymbol{F}_\xi+(\boldsymbol{\zeta}_{\rm a}\cdot\nabla\theta_{\rm e})Q_{\rm n}\ ,\end{aligned} \qquad (2.10)$$

where

$$(\boldsymbol{\zeta}_{\rm a}\cdot\nabla\theta_{\rm e})Q_{\rm n}$$

is the contribution of mass forcing caused by precipitation and condensation to the variation of MPV.

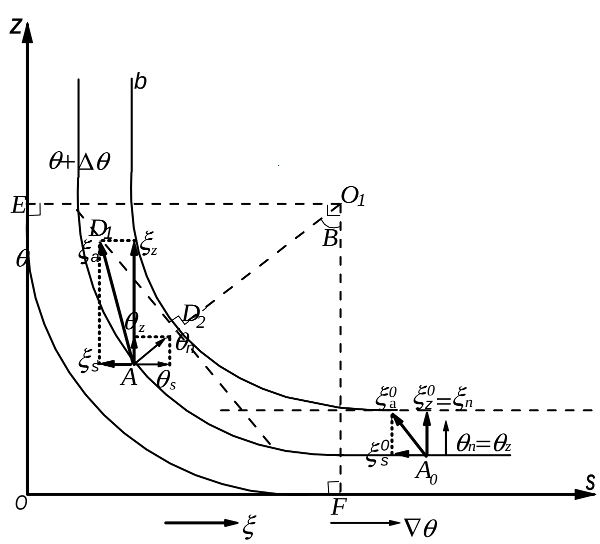


**Fig. 1.** Schematic diagram of USVD.

## 3. The theory of USVD

Based on the conservation of Ertel PV and MPV, Wu et al. (1998) advanced the theory of SVD. Since there are often apparent slantwise up-sliding motions immediately in front of severe storms, such as oceanic cyclones and rainstorms in the downwind direction, seen from both observations and numerical simulations (Zhang et al., 1999; Cui, 2001), a deduction, the theory of USVD, is proposed and described below in detail. The Z-coordinate is adopted here. USVD is described in Fig. 1, where we assume that the parallel isentropic surfaces are horizontal or perpendicular outside the box $\rm OFO_1E$, but are bent as circles inside the box. For simplicity, we further assume that the gradient of the isentropic surfaces,

$$\triangle\theta=\theta_{\rm n}$$

is constant. And also a circle 'b' is defined, which is coaxial with the isentropic surfaces and keeps from

$$\theta+\triangle\theta$$

at a constant distance $\mid\xi_{\rm n}\mid$. From the definition of Ertel PV, we get

$$P_{\rm E}=\xi_{\rm n}\theta_{\rm n}=\xi_z\theta_z+\xi_{\rm s}\theta_{\rm s} \qquad (3.1)$$

and further,

$$\xi_z=\frac{\xi_{\rm n}\theta_{\rm n}-\xi_{\rm s}\theta_{\rm s}}{\theta_z}=\frac{P_{\rm E}-\xi_{\rm s}\theta_{\rm s}}{\theta_z}\ ,\ \ (\theta_z\neq0) \qquad (3.2)$$

where

$$\xi_{\rm n}=\alpha\zeta_{\rm n}$$

is the projection of

$$\boldsymbol{\xi}_{\rm a}=\alpha\boldsymbol{\zeta}_{\rm a}$$

on $\boldsymbol{n}$ ($\boldsymbol{n}$ is the direction of $-\nabla\theta$), and

$$\xi_z=\alpha\zeta_z\quad\text{and}\quad\xi_{\rm s}=\alpha\zeta_{\rm s}\ ,$$

are the vertical and horizontal components of $\boldsymbol{\xi}_{\rm a}$, respectively;

$$\theta_{\rm n}=\mid\nabla\theta\mid,$$

and $\theta_{\rm s}$ and $\theta_z$, are the horizontal and vertical components of $\theta_{\rm n}$, respectively. Here $\alpha=\rho^{-1}$, and $\rho$ is air density; $\boldsymbol{\zeta}_{\rm a}$ is absolute vorticity, and $\zeta_s$ and $\zeta_z$ are the horizontal and vertical components of $\boldsymbol{\zeta}_{\rm a}$, respectively.

For an air parcel $\rm A_0$ moving on the isentropic surface $\theta+\triangle\theta$ leftward, when outside the box $\rm OFO_1E$, $\zeta_z$ does not vary according to the BOX law (Wu et al., 1998) no matter what

$$\xi_{\rm s}=\alpha\zeta_{\rm s}=\alpha\partial V_{\rm m}/\partial z$$

is. When $\rm A_0$ continues to move leftward on the isentropic surface $\theta+\triangle\theta$ into the box by sliding up an angle $B$ ($B$ is positive when one side deviates from

$-z$ towards $-S$) to point A, the head point $D_1$ of $\boldsymbol{\xi}_a$ of the parcel $A_0$ should be located in a plane $D_1D_2$ which is a tangential plane to circle 'b' at point $D_2$ as shown in Fig. 1 according to the CIRCUMSCRIBED PLANE law (Wu et al., 1998). Because, according to the figure,

$$\tan B = \frac{\theta_s}{\theta_z}\ , \quad \left(-\frac{\pi}{2} < B < \frac{\pi}{2}\right) \tag{3.3}$$

and $\boldsymbol{n}\cdot\boldsymbol{k} > 0$, then

$$\cos B = \frac{\theta_z}{\theta_n} > 0\ . \tag{3.4}$$

Introducing them into (3.2), we get

$$\xi_z = \frac{\xi_n}{\cos B} - \xi_s \tan B\ , \quad \left(\mid B \mid \neq \frac{\pi}{2}\right) \tag{3.5}$$

In the Northern Hemisphere in the case of cyclogenesis, we get $\xi_n > 0$. If the following condition is satisfied:

$$C_D = \frac{\xi_s\theta_s}{\theta_z} < 0\ , \tag{3.6}$$

then (3.5) could be rewritten as

$$\xi_z = \frac{\xi_n}{\cos B} + \mid \xi_s \tan B \mid\ , \quad \left(\mid B \mid \neq \frac{\pi}{2}\right) \tag{3.7}$$

where $\xi_z$ increases with increasing $\mid B \mid$. When (3.6) is satisfied (when point $A_0$ is outside the box, $\theta_s = 0$, so originally $C_D$ equals 0; then (3.6) is equivalent to $dC_D/dt < 0$), the vertical component of absolute vorticity of parcel $A_0$ should grow, and when the isentropic surfaces are sharply steep, $\xi_z$ becomes very large:

$$\xi_z \to \infty\ , \quad |B| \to \frac{\pi}{2}\ .$$

Because the development of vorticity is due to the upsliding of the air parcel along a slantwise isentropic surface, it can be referred to as USVD. Apparently, USVD will not occur unless three conditions are satisfied, namely, the presence of slantwise isentropic surfaces (or moist isentropic surfaces for moist air), upsliding slantwise motions on isentropic surfaces, and $dC_D/dt < 0$ (or $dC_m/dt < 0$ for moist air).

## 4. Complete vorticity equation

Upon applying the total derivative to both sides of (3.2), the complete vorticity equation for dry air can be obtained as

$$\frac{D\zeta_z}{Dt} + \beta v + (f+\zeta_z)\nabla\cdot\boldsymbol{V} = \frac{1}{a}\frac{D}{Dt}\left[\frac{P_E}{\theta_z} - C_D\right]\ ,$$
$$\theta_z \neq 0 \tag{4.1}$$

where $P_E$ is the Ertel PV,

$$C_D = \frac{\xi_s\theta_s}{\theta_z}$$

is the dry SVD index, and $\theta_z$ is the vertical component of the gradient of potential temperature.

If moist air is studied, then the corresponding equation for moist air can be obtained as

$$\frac{D\zeta_z}{Dt} + \beta v + (f+\zeta_z)\nabla\cdot\boldsymbol{V} = \frac{1}{a}\frac{D}{Dt}\left[\frac{P_m}{\theta_{ez}} - C_m\right]$$
$$-\frac{Q_n(\zeta_z+f)}{\alpha}\ , \quad \theta_{ez} \neq 0 \tag{4.2}$$

where $P_m$ is MPV,

$$C_m = \frac{\xi_s\theta_{es}}{\theta_{ez}}$$

is the corresponding moist SVD index, and $\theta_{ez}$ is the vertical component of the gradient of equivalent potential temperature.

## 5. Comparison between the complete vorticity equation and the traditional vorticity equation

Compared to the traditional vorticity equation, the complete vorticity equation explicitly covers the effects of both internal forcings, such as variations of stability, baroclinicity, and vertical shear of horizontal wind, and external forcings, such as diabatic heating, friction, and mass forcing, thus making it more suitable for application. Below is the comparison between these two equations in detail.

The horizontal air dynamic equation set can be written as

$$\frac{du}{dt} = -\alpha\frac{\partial p}{\partial x} + fv - \tilde{f}w + F_x\ , \tag{5.1}$$

$$\frac{dv}{dt} = -\alpha\frac{\partial p}{\partial y} - fu + F_y\ . \tag{5.2}$$

By omitting $\tilde{f}w$ and applying the partial derivative operators of $x$ and $y$ to (5.2) and (5.1), respectively, and subtracting the derivative of (5.1) from that of (5.2), we get the traditional vorticity equation

$$\frac{d\varsigma_z}{dt} + \beta v + (f+\varsigma_z)\,\nabla\cdot\boldsymbol{V} = (f+\varsigma_z)\frac{\partial w}{\partial z}$$
$$+\left(\frac{\partial u}{\partial z}\frac{\partial w}{\partial y} - \frac{\partial v}{\partial z}\frac{\partial w}{\partial x}\right) + N_z + \boldsymbol{k}\cdot\boldsymbol{F}_\xi\ , \tag{5.3}$$

where the four terms on the right side are the stretching term, the twisting term, the horizontal solenoid term

$$N_z = \frac{\partial p}{\partial x}\frac{\partial \alpha}{\partial y} - \frac{\partial p}{\partial y}\frac{\partial \alpha}{\partial x}\ ,$$

and the vertical component of eddy friction diffusion, respectively.

From the definition of MPV and moist SVD index, we get

$$P_m = \xi_s\theta_{es} + \xi_z\theta_{ez}\ ,$$

$$C_{\rm m} = \frac{\xi_{\rm s}\theta_{\rm es}}{\theta_{\rm ez}} \, .$$

Introducing (2.9), (2.10), and the above two expressions into(4.2), we get the complete vorticity equation with mass forcing as

$$\begin{aligned}
&\frac{d\zeta_z}{dt} + \beta v + (f+\zeta_z)\nabla\cdot\boldsymbol{V} = \\
&-\frac{1}{\alpha\theta_{\rm ez}^2}\left[(P_{\rm m}-\xi_{\rm s}\theta_{\rm es})\frac{d\theta_{\rm ez}}{dt} + \theta_{\rm ez}\xi_{\rm s}\frac{d\theta_{\rm es}}{dt} + \theta_{\rm es}\theta_{\rm ez}\frac{d\xi_{\rm s}}{dt}\right] \\
&+\frac{1}{\theta_{\rm ez}}\nabla\theta_{\rm e}\cdot\boldsymbol{F}_\xi + \frac{1}{\theta_{\rm ez}}\boldsymbol{\zeta}_{\rm a}\cdot\nabla Q + \frac{(\nabla p\times\nabla\alpha)\cdot\nabla\theta_{\rm e}}{\theta_{\rm ez}} \\
&+\frac{(\boldsymbol{\zeta}_{\rm a}\cdot\nabla\theta_{\rm e})Q_{\rm n}}{\alpha\theta_{\rm ez}} - \frac{Q_{\rm n}(\zeta_z+f)}{\alpha} \quad (\theta_{\rm ez}\neq 0) \, .
\end{aligned} \tag{5.4}$$

For

$$\xi_z = \alpha(\zeta_z + f)$$

and

$$\xi_{\rm s} = \alpha\zeta_{\rm s}$$

the above equation can be rewritten as

$$\begin{aligned}
&\frac{d\zeta_z}{dt} + \beta v + (f+\zeta_z)\nabla\cdot\boldsymbol{V} = \\
&\left[\frac{(f+\zeta_z)}{\theta_{\rm ez}}\left(-\frac{d\theta_{\rm ez}}{dt} + \frac{\partial Q}{\partial z}\right) + \frac{\zeta_{\rm s}}{\theta_{\rm ez}}\left(-\frac{d\theta_{\rm es}}{dt} + \frac{\partial Q}{\partial s}\right)\right. \\
&\left.+\frac{1}{\theta_{\rm ez}}\nabla\theta_{\rm e}\cdot\boldsymbol{F}_\xi\right] + \left[-\frac{\theta_{\rm es}}{\alpha\theta_{\rm ez}}\frac{d\alpha\zeta_{\rm s}}{dt} + \frac{(\nabla p\times\nabla\alpha)\cdot\nabla\theta_{\rm e}}{\theta_{\rm ez}}\right] \\
&+\frac{\zeta_{\rm s}\theta_{\rm es}Q_{\rm n}}{\alpha\theta_{\rm ez}} \quad (\theta_{\rm ez}\neq 0) \, .
\end{aligned} \tag{5.5}$$

And it can be further expressed as

$$\begin{aligned}
&\frac{d\zeta_z}{dt} + \beta v + (f+\zeta_z)\nabla\cdot\boldsymbol{V} = \\
&\left[\frac{(f+\zeta_z)}{\theta_{\rm ez}}\left(-\frac{d\theta_{\rm ez}}{dt} + \frac{\partial Q}{\partial z}\right) + \frac{\zeta_x}{\theta_{\rm ez}}\left(-\frac{d\theta_{\rm ex}}{dt} + \frac{\partial Q}{\partial x}\right)\right. \\
&\left.+\frac{\zeta_y}{\theta_{\rm ez}}\left(-\frac{d\theta_{\rm ey}}{dt} + \frac{\partial Q}{\partial y}\right) + \frac{1}{\theta_{\rm ez}}\nabla\theta_{\rm e}\cdot\boldsymbol{F}_\xi\right] \\
&+\left[-\frac{\theta_{\rm es}}{\alpha\theta_{\rm ez}}\frac{d\alpha\zeta_{\rm s}}{dt} + \frac{(\nabla p\times\nabla\alpha)\cdot\nabla\theta_{\rm e}}{\theta_{\rm ez}}\right] \\
&+\frac{\zeta_{\rm s}\theta_{\rm es}Q_{\rm n}}{\alpha\theta_{\rm ez}} \quad (\theta_{\rm ez}\neq 0) \, .
\end{aligned} \tag{5.6}$$

We have the derivative relation

$$\frac{d\theta_{\rm ez}}{dt} = \frac{\partial}{\partial t}\left(\frac{\partial\theta_{\rm e}}{\partial z}\right) + \boldsymbol{V}\cdot\nabla\frac{\partial\theta_{\rm e}}{\partial z} \, . \tag{5.7}$$

Then we get

$$\frac{d\theta_{\rm ez}}{dt} = \frac{\partial}{\partial z}\left(\frac{d\theta_{\rm e}}{dt}\right) - \nabla\theta_{\rm e}\cdot\frac{\partial\boldsymbol{V}}{\partial z} \, . \tag{5.8}$$

For the same reason, we get

$$\frac{d\theta_{\rm ex}}{dt} = \frac{\partial}{\partial x}\left(\frac{d\theta_{\rm e}}{dt}\right) - \nabla\theta_{\rm e}\cdot\frac{\partial\boldsymbol{V}}{\partial x} \, , \tag{5.9a}$$

$$\frac{d\theta_{\rm ey}}{dt} = \frac{\partial}{\partial y}\left(\frac{d\theta_{\rm e}}{dt}\right) - \nabla\theta_{\rm e}\cdot\frac{\partial\boldsymbol{V}}{\partial y} \, . \tag{5.9b}$$

By introducing (5.8), (5.9), and (2.3) into (5.6), we obtain

$$\begin{aligned}
&\frac{d\zeta_z}{dt} + \beta v + (f+\zeta_z)\nabla\cdot\boldsymbol{V} = \\
&\left[\frac{(f+\zeta_z)}{\theta_{\rm ez}}\left(\nabla\theta_{\rm e}\cdot\frac{\partial\boldsymbol{V}}{\partial z}\right) + \frac{\zeta_x}{\theta_{\rm ez}}\left(\nabla\theta_{\rm e}\cdot\frac{\partial\boldsymbol{V}}{\partial x}\right)\right. \\
&\left.+\frac{\zeta_y}{\theta_{\rm ez}}\left(\nabla\theta_{\rm e}\cdot\frac{\partial\boldsymbol{V}}{\partial y}\right) + \frac{1}{\theta_{\rm ez}}\nabla\theta_{\rm e}\cdot\boldsymbol{F}_\xi\right] \\
&+\left[-\frac{\theta_{\rm es}}{\alpha\theta_{\rm ez}}\frac{d\alpha\zeta_{\rm s}}{dt} + \frac{(\nabla p\times\nabla\alpha)_{\rm s}\theta_{\rm es}}{\theta_{\rm ez}} + N_z\right] \\
&+\frac{\zeta_{\rm s}\theta_{\rm es}Q_{\rm n}}{\alpha\theta_{\rm ez}} \quad (\theta_{\rm ez}\neq 0) \, ,
\end{aligned} \tag{5.10}$$

where

$$(\nabla p\times\nabla\alpha)_{\rm s}$$

is the horizontal component of the solenoid term. Further we have

$$\begin{aligned}
&\frac{d\zeta_z}{dt} + \beta v + (f+\zeta_z)\nabla\cdot\boldsymbol{V} = \\
&\left\{\left[(f+\zeta_z)\frac{\partial w}{\partial z} + \zeta_s\frac{\partial w}{\partial s}\right] + \boldsymbol{k}\cdot\boldsymbol{F}_\xi\right\} \\
&+\left[\frac{(f+\zeta_z)}{\theta_{\rm ez}}\theta_{\rm es}\frac{\partial V_{\rm s}}{\partial z} + \frac{\zeta_x}{\theta_{\rm ez}}\theta_{\rm es}\frac{\partial V_{\rm s}}{\partial x} + \frac{\zeta_y}{\theta_{\rm ez}}\theta_{\rm es}\frac{\partial V_{\rm s}}{\partial y}\right. \\
&\left.+\frac{1}{\theta_{\rm ez}}(\theta_{\rm es}F_{\xi{\rm s}})\right] + \left[-\frac{\theta_{\rm es}}{\alpha\theta_{\rm ez}}\frac{d\alpha\zeta_{\rm s}}{dt} + \frac{(\nabla p\times\nabla\alpha)_{\rm s}\theta_{\rm es}}{\theta_{\rm ez}} + N_z\right] \\
&+\frac{\zeta_{\rm s}Q_{\rm n}\theta_{\rm es}}{\alpha\theta_{\rm ez}} \quad (\theta_{\rm ez}\neq 0) \, .
\end{aligned} \tag{5.11}$$

Comparing the complete vorticity equation (5.11) with the traditional vorticity equation (5.3), we find that the former contains some extra terms not included in the latter:

(1) $$\underbrace{\frac{(f+\zeta_z)}{\theta_{\rm ez}}\theta_{\rm es}\frac{\partial V_{\rm s}}{\partial z}}_{\rm A} + \underbrace{\frac{\zeta_x}{\theta_{\rm ez}}\theta_{\rm es}\frac{\partial V_{\rm s}}{\partial x}}_{\rm B} + \underbrace{\frac{\zeta_y}{\theta_{\rm ez}}\theta_{\rm es}\frac{\partial V_{\rm s}}{\partial y}}_{\rm C} + \underbrace{\frac{1}{\theta_{\rm ez}}(\theta_{\rm es}F_{\xi{\rm s}})}_{\rm D}$$

(2) $$\underbrace{-\frac{\theta_{\rm es}}{\alpha\theta_{\rm ez}}\frac{d\alpha\zeta_{\rm s}}{dt}}_{\rm E} + \underbrace{\frac{(\nabla p\times\nabla\alpha)_{\rm s}\theta_{\rm es}}{\theta_{\rm ez}}}_{\rm F} + \underbrace{\frac{\zeta_{\rm s}Q_{\rm n}\theta_{\rm es}}{\alpha\theta_{\rm ez}}}_{\rm G}$$

where A, B, and C represent the vertical, $X$- and $Y$-components of the vorticity advection of horizontal

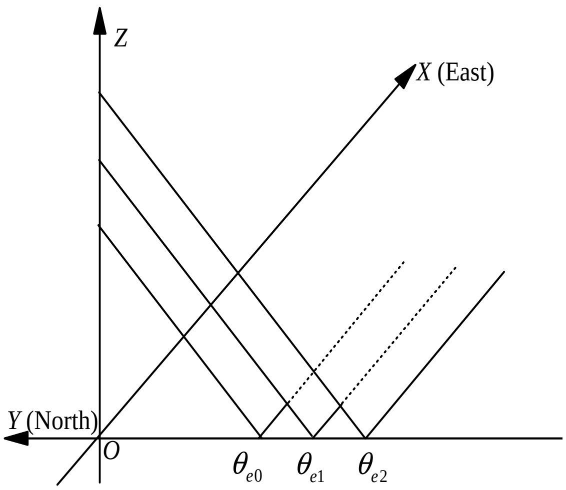


**Fig. 2.** Simplified Changjiang-Huaihe Meiyu front model.

velocity respectively, D represents the contribution of the horizontal component of eddy friction diffusion, E is the contribution of the variation of the vertical shear of horizontal velocity, F is the horizontal component of the solenoid term, and G is the contribution of mass forcing.

The common feature of the above seven terms is that they are all closely related to the slope of moist isentropic surfaces

$$\tan\delta = \theta_{\mathrm{es}}/\theta_{\mathrm{e}z}\ .$$

When the surfaces are flat,

$$\theta_{\mathrm{es}} \approx 0 \quad \text{and} \quad \tan\delta = \theta_{\mathrm{es}}/\theta_{\mathrm{e}z} = 0\ ;$$

then all of the above seven terms equal zero, and the complete vorticity equation is identical to the traditional counterpart. Below, the physical interpretations of some of the extra terms will be presented by taking a simplified Changjiang-Huaihe Meiyu front model as an example. For simplicity, the parallel moist isentropic surfaces are set to be parallel to the $x$-coordinate (Fig. 2). Assuming $\nabla\theta_{\mathrm{e}}$=constant, we get $\theta_{\mathrm{e}x} = 0$; from Fig. 2 we also get $\theta_{\mathrm{ey}} < 0$ and $\theta_{\mathrm{e}z} > 0$; further we assume that the gradients of all kinds of variables are zero in the X-direction, that is, $\partial/\partial x \equiv 0$. From the thermal-wind equation, we get

$$\frac{\partial u}{\partial z} \propto -\frac{\partial T}{\partial y} > 0$$

and

$$\frac{\partial v}{\partial z} \propto \frac{\partial T}{\partial x} = 0$$

at last we assume that the horizontal shear of vertical velocity is far less than the vertical shear of horizontal velocity.

Then the above seven terms can be rewritten as

$$\mathrm{A}:\ \frac{(f+\zeta_z)}{\theta_{\mathrm{e}z}}\theta_{\mathrm{es}}\frac{\partial V_{\mathrm{s}}}{\partial z} = \frac{(f+\zeta_z)}{\theta_{\mathrm{e}z}}\left(\theta_{\mathrm{e}x}\frac{\partial u}{\partial z} + \theta_{\mathrm{ey}}\frac{\partial v}{\partial z}\right) = 0\ ,$$

$$\mathrm{B}:\ \frac{\zeta_x}{\theta_{\mathrm{e}z}}\theta_{\mathrm{es}}\frac{\partial V_{\mathrm{s}}}{\partial x} = \frac{1}{\theta_{\mathrm{e}z}}\left(\frac{\partial w}{\partial y} - \frac{\partial v}{\partial z}\right)\left(\theta_{\mathrm{e}x}\frac{\partial u}{\partial x} + \theta_{\mathrm{ey}}\frac{\partial v}{\partial x}\right) = 0\ ,$$

$$\mathrm{C}:\ \frac{\zeta_y}{\theta_{\mathrm{e}z}}\theta_{\mathrm{es}}\frac{\partial V_{\mathrm{s}}}{\partial y} = \frac{1}{\theta_{\mathrm{e}z}}\left(\frac{\partial u}{\partial z} - \frac{\partial w}{\partial x}\right)\left(\theta_{\mathrm{e}x}\frac{\partial u}{\partial y} + \theta_{\mathrm{ey}}\frac{\partial v}{\partial y}\right) = \frac{\theta_{\mathrm{ey}}}{\theta_{\mathrm{e}z}}\left(\frac{\partial u}{\partial z}\right)\left(\frac{\partial v}{\partial y}\right)\ ,$$

$$\mathrm{D}:\ \frac{1}{\theta_{\mathrm{e}z}}(\theta_{\mathrm{es}}F_{\xi\mathrm{s}}) = \frac{\theta_{\mathrm{e}x}F_{\xi x}}{\theta_{\mathrm{e}z}} + \frac{\theta_{\mathrm{ey}}F_{\xi y}}{\theta_{\mathrm{e}z}} = \frac{\theta_{\mathrm{ey}}F_{\xi y}}{\theta_{\mathrm{e}z}}\ ,$$

$$\mathrm{E}:\ -\frac{\theta_{\mathrm{es}}}{\alpha\theta_{\mathrm{e}z}}\frac{d\alpha\zeta_{\mathrm{s}}}{dt} = -\frac{\theta_{\mathrm{e}x}}{\alpha\theta_{\mathrm{e}z}}\frac{d[\alpha(\partial w/\partial y - \partial v/\partial z)]}{dt} - \frac{\theta_{\mathrm{ey}}}{\alpha\theta_{\mathrm{e}z}}\frac{d[\alpha(\partial u/\partial z - \partial w/\partial x)]}{dt} = -\frac{\theta_{\mathrm{ey}}}{\alpha\theta_{\mathrm{e}z}}\frac{d[\alpha(\partial u/\partial z)]}{dt}\ ,$$

$$\mathrm{F}:\ \frac{(\nabla p\times\nabla\alpha)_{\mathrm{s}}\theta_{\mathrm{es}}}{\theta_{\mathrm{e}z}} = \frac{\theta_{\mathrm{e}x}}{\theta_{\mathrm{e}z}}\left(\frac{\partial p}{\partial y}\frac{\partial\alpha}{\partial z} - \frac{\partial p}{\partial z}\frac{\partial\alpha}{\partial y}\right) + \frac{\theta_{\mathrm{ey}}}{\theta_{\mathrm{e}z}}\left(\frac{\partial p}{\partial z}\frac{\partial\alpha}{\partial x} - \frac{\partial p}{\partial x}\frac{\partial\alpha}{\partial z}\right) = 0\ ,$$

$$\mathrm{G}:\ \frac{\zeta_{\mathrm{s}}Q_{\mathrm{n}}\theta_{\mathrm{es}}}{\alpha\theta_{\mathrm{e}z}} = \frac{Q_{\mathrm{n}}\theta_{\mathrm{e}x}}{\alpha\theta_{\mathrm{e}z}}\left(\frac{\partial w}{\partial y} - \frac{\partial v}{\partial z}\right) + \frac{Q_{\mathrm{n}}\theta_{\mathrm{ey}}}{\alpha\theta_{\mathrm{e}z}}\left(\frac{\partial u}{\partial z} - \frac{\partial w}{\partial x}\right) = \frac{Q_{\mathrm{n}}\theta_{\mathrm{ey}}}{\alpha\theta_{\mathrm{e}z}}\left(\frac{\partial u}{\partial z}\right)\ .$$

In this case, C, D, E, and G are not zero. (The physical interpretations of the other three terms and the eddy friction diffusion D will be discussed in another paper.) In detail, as to C, when there is convergence in the Y direction

$$\frac{\partial v}{\partial y} < 0$$

since,

$$\frac{\partial u}{\partial z} > 0,\ \theta_{\mathrm{ey}} < 0\ ,\ \text{and}\ \theta_{\mathrm{e}z} > 0\ ,$$

then, $C > 0$, which means that the vertical component of vorticity will increase. In fact, the convergences and divergences are just representing the respective procedures of frontogenesis and frontolysis (Fig. 2). In the term of E, since,

$$\theta_{\mathrm{ey}} < 0,\ \theta_{\mathrm{e}z} > 0$$

and according to the thermal-wind relation

$$\frac{d[\alpha(\partial u/\partial z)]}{dt} \propto -\frac{d[\alpha(\partial T/\partial y)]}{dt}\ ,$$

when the temperature gradient in the $Y$ direction increases, that is, the baroclinity increases, $E > 0$, the vertical vorticity will increase. As for G, when it is raining, we have, $Q_{\rm n} > 0$ and since,

$$\frac{\partial u}{\partial z} > 0,\ \ \theta_{\rm ey} < 0 \text{ , and } \theta_{\rm ez} > 0 \text{ ,}$$

then, $G < 0$, and the vertical vorticity will decrease. From the above we know that frontogenesis and the increase of baroclinicity are favorable to the development of vertical vorticity, while mass forcing is disfavorable to it.

Here only three terms of the seven extra terms are analyzed, but we can also find out that near slantwise isentropic surfaces, the variations of some thermodynamic terms and mass forcing are important to the development of vorticity as being set forth in the theory of SVD and USVD and should not be ignored. Certainly, to use the complete vorticity equation and the theory to investigate synoptic systems, a closer analysis of the physical interpretations of the seven extra terms is needed, which will be done in another paper. Furthermore, since the evolution of vertical vorticity results from many factors in synthesis, any analysis results from one or part of the factors are partial. It is notable that the complete vorticity equation just provides a proper method to do vorticity analyses; one form of the complete vorticity equation, (4.1) and (4.2), give us a solution to study the evolution of vertical vorticity in synthesis, while the other form, (5.11), provides an approach to study the effect of each factor respectively.

## 6. Qualitative analyses of the up-sliding slantwise vorticity development of "June 1999" rainstorm in the Changjiag-Huaihe region

Mesoscale systems often occur along the Changjiang-Huaihe Meiyu front in the summer, which frequently bring together heavy rains or torrential rains. The prediction of these kind of systems is very important to the forecasts of torrential rains in Changjiag-Huaihe valley. Here a 60-h simulation is performed to reproduce a torrential rain event near the Changjiag-Huaihe Meiyu front during 22–44 June 1999, and the model output is analyzed.

The PSU/NCAR three-dimensional, nonhydrostatic, nested-grid, mesoscale model (MM5V2) is used for the present simulation. The fundamental features of the model used include: (1) a two-way interactive nested-grid procedure (Fig. 3); (2) use of the Kain-Fritsch cumulus parameterization scheme for the fine-mesh domain and the Anthes-type cumulus scheme for the coarse-mesh domain; (3) an explicit Reisner2 moisture scheme for both coarse and fine-mesh domains; and (4) the Blackadar high-resolution boundary-layer parameterization.

The nested-grid ratio is 1 to 3, with a fine-mesh length of 25 km and a coarse-mesh length of 75 km. The $(x \times y \times \delta)$ dimensions of the coarse and fine meshes are $70 \times 61 \times 23$ and $130 \times 106 \times 23$ respectively, and they are overlaid on a LAMBERT map projection true at 30°N and 60°N. The 24 $\delta$-levels are 0.0, 0.05, 0.1, 0.15, 0.2, 0.25, 0.3, 0.35, 0.4, 0.45, 0.5, 0.55, 0.6, 0.65, 0.7, 0.75, 0.8, 0.85, 0.89, 0.93, 0.96, 0.98, 0.99, and 1.0. The use of an interactive two-way nested grid is helpful for solving the boundary problem of regional models. And the pressure at the top of the model atmosphere is 70 hPa. The model is initialized at 0000 UTC 22 June 1999 with data from the NCEP 2.5° latitude-longitude global reanalysis and rawinsonde observations. The model domains, and topography are shown in Fig. 3.

By comparing the output with the observations (Fig. 4), we find that the model reproduces well the evolution of the mesoscale systems. Figure 4 shows the observational and simulated sea-level pressure, in which both the intensification and the movement of the mesoscale systems are reproduced well, so the model output can be used for further diagnosis. Based on the theory of USVD, the torrential rain is analyzed below qualitatively with the high-resolution model output in the context of slantwise isentropic surfaces to demonstrate the application of USVD and the complete vorticity equation proposed above. (For economy of space, only sea-level pressure is verified against observations. Detailed verifications and qualitative and

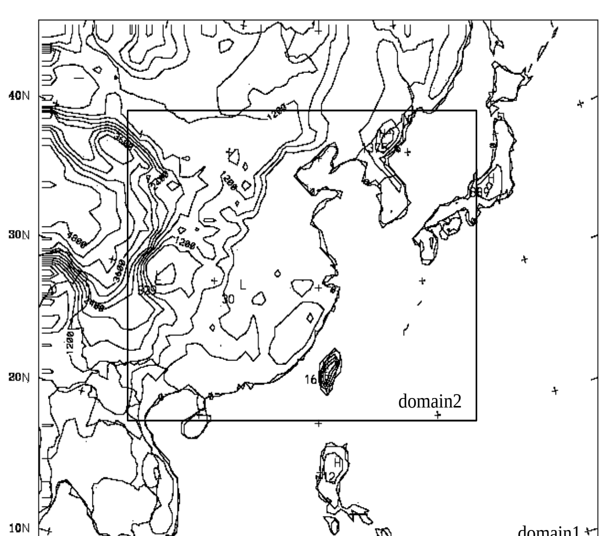


**Fig. 3.** Model domains and topography.

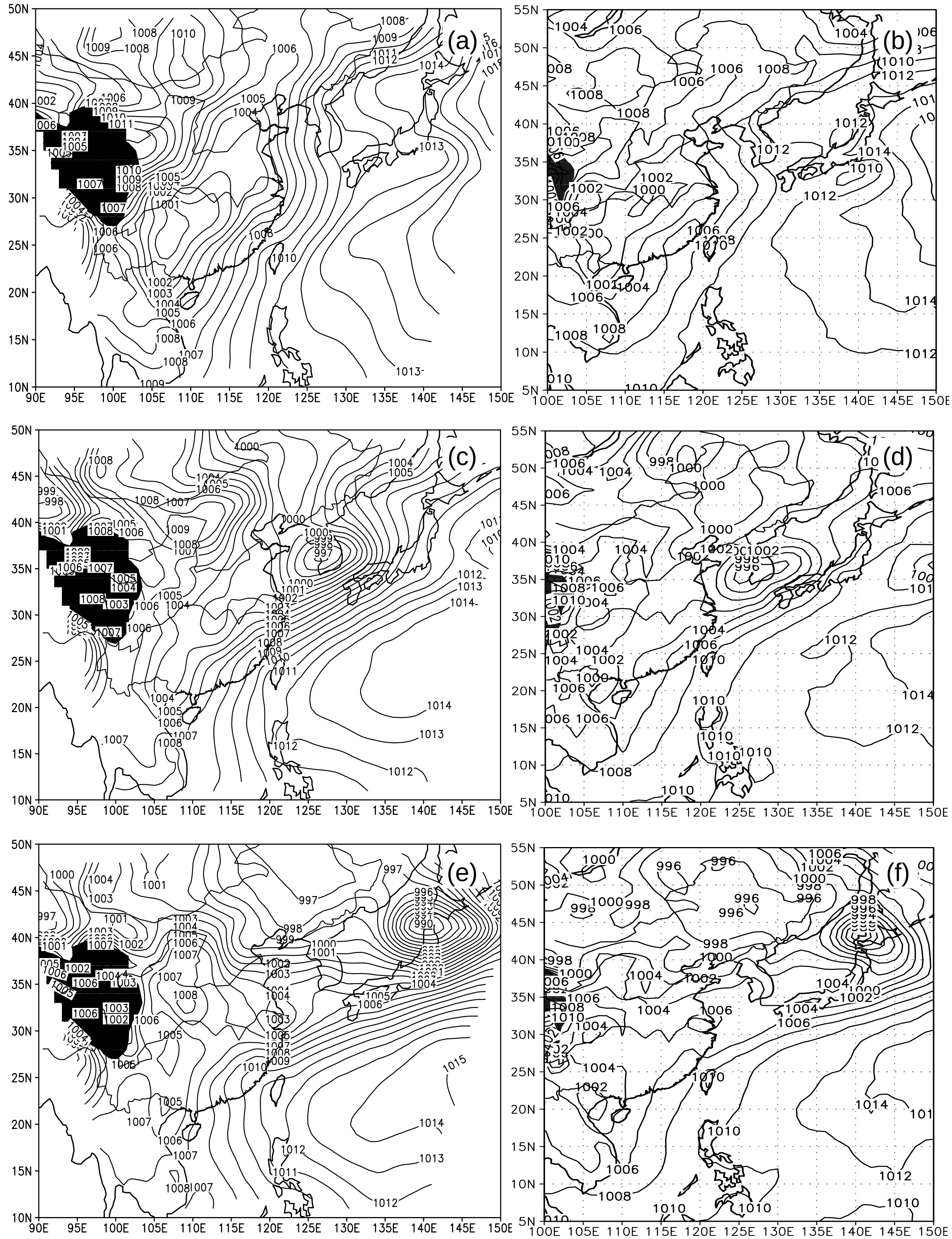


**Fig. 4.** Sea-Level Pressure (SLP, hPa); shading denotes topography > 3000 m. (a), (c), and (e) from simulation; (b), (d), and (f) from observations; (a), (b) 1200 UTC 22 June; (c), (d) 1200 UTC 23 June; (e), (f) 1200 UTC 24 June.

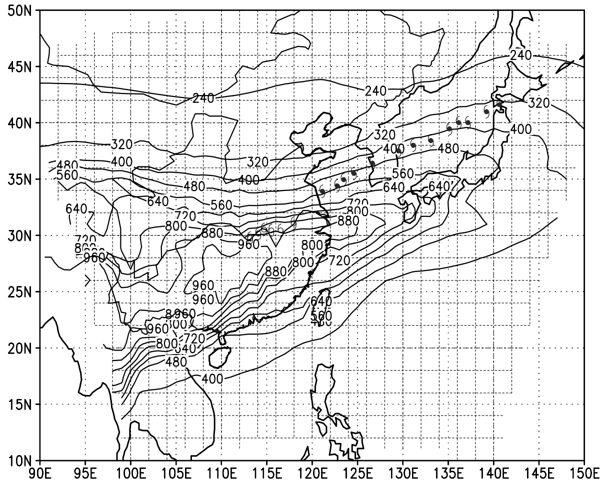


**Fig. 5.** 60-h averaged pressures and tracks of the mesoscale systems during model time on the 340 K moist isentropic surface.

quantitative analyses of USVD will be discussed in another paper.)

Figure 5 gives the 60-h average pressures and tracks of two apparent mesoscale cyclones during model time on a 340 K moist isentropic surface. The 340 K moist isentropic surface is shaped like a funnel with higher pressures in the center and lower ones outside. There are two evident belts of concentrated isopiestics: the northern one lies between 30°–38°N approximately in an East-West direction, which denotes the position of the Changjiang-Huaihe Meiyu front; the southern one lies between 15°–28°N in an approximately northeast-southwest direction, which is related to the Subtropical High. The two concentrated belts form the so-called Changjiang-Huaihe Meiyu Front System first introduced in the observational analysis of Zhou et al. (2001). The stronger mesoscale cyclone(denoted by a solid cyclonic symbol in Fig. 5, hereafter referred to as D1) reaches the ocean to the south of the Jiao-Dong Peninsula and moves on to the Japanese Sea in a slightly northeast-southwest direction. At the end of the simulation, it arrives at the sea to the west of Japan near (41°N, 139°E) with a span of central sea level pressure from 1002 hPa to 990 hPa and a pressure-fall rate of 14 hPa/30 h; The rate obtains its peak value(3 hPa/3 h) during 1500–1800 UTC 23 June. The weaker mesoscale cyclone (denoted by a hollow cyclonic symbol in Fig. 5, hereafter referred to as D2) develops and moves slowly along the valley of the Yangtze River during the simulation. The common property of these two cyclones is that both occur and develop near the northern branch of the Changjiang-Huaihe Meiyu Front System, that is, the Changjiang-Huaihe Meiyu front, which is identical to the findings of Wu et al. (1995). Below, only D1 will be investigated for simplicity.

Figure 6 shows the meridional cross-sections across the centers of daily precipitation greater than 50 mm 23 June. Solid lines are for equivalent potential temperature, and thin lines for positive vorticity. In the figure, positive vorticities always lie near the slantwise moist isentropic surfaces of the Meiyu front; cold and warm air converge remarkably near the slantwise moist isentropic surfaces with strong up-sliding motions and consequent heavy rains, which is identical to the analyses above. According to section 3, USVD will not

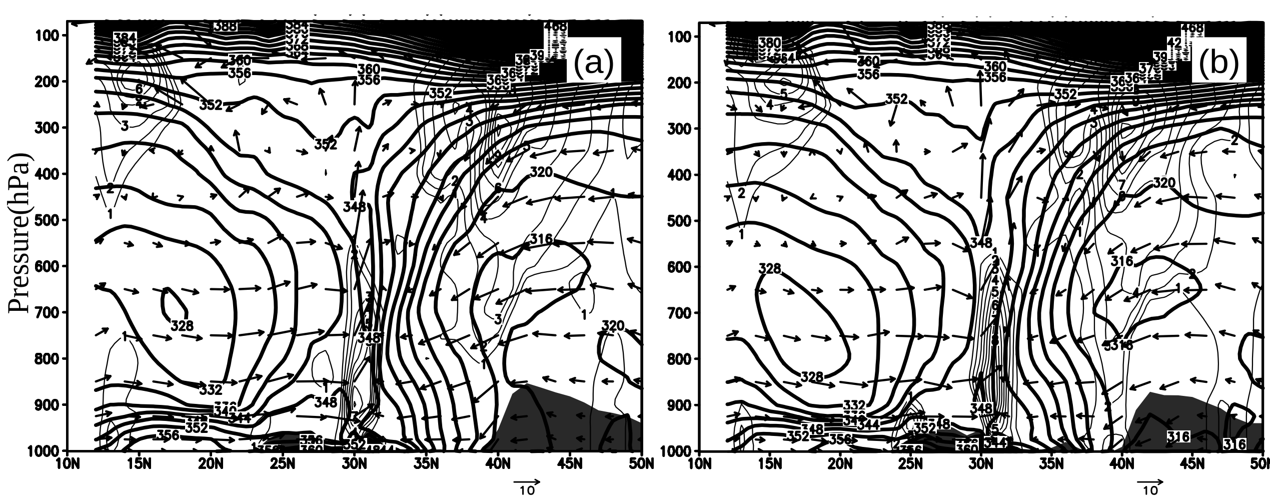


**Fig. 6.** Meridional cross-sections across the centers of daily precipitation greater than 50 mm (23 June Solid lines are for equivalent potential temperature, thin lines for positive vorticity in units of $10^{-5}$ s$^{-1}$. The shaded area denotes topography. (a) 23 June along 116°E; (b) 23 June along 118°E.

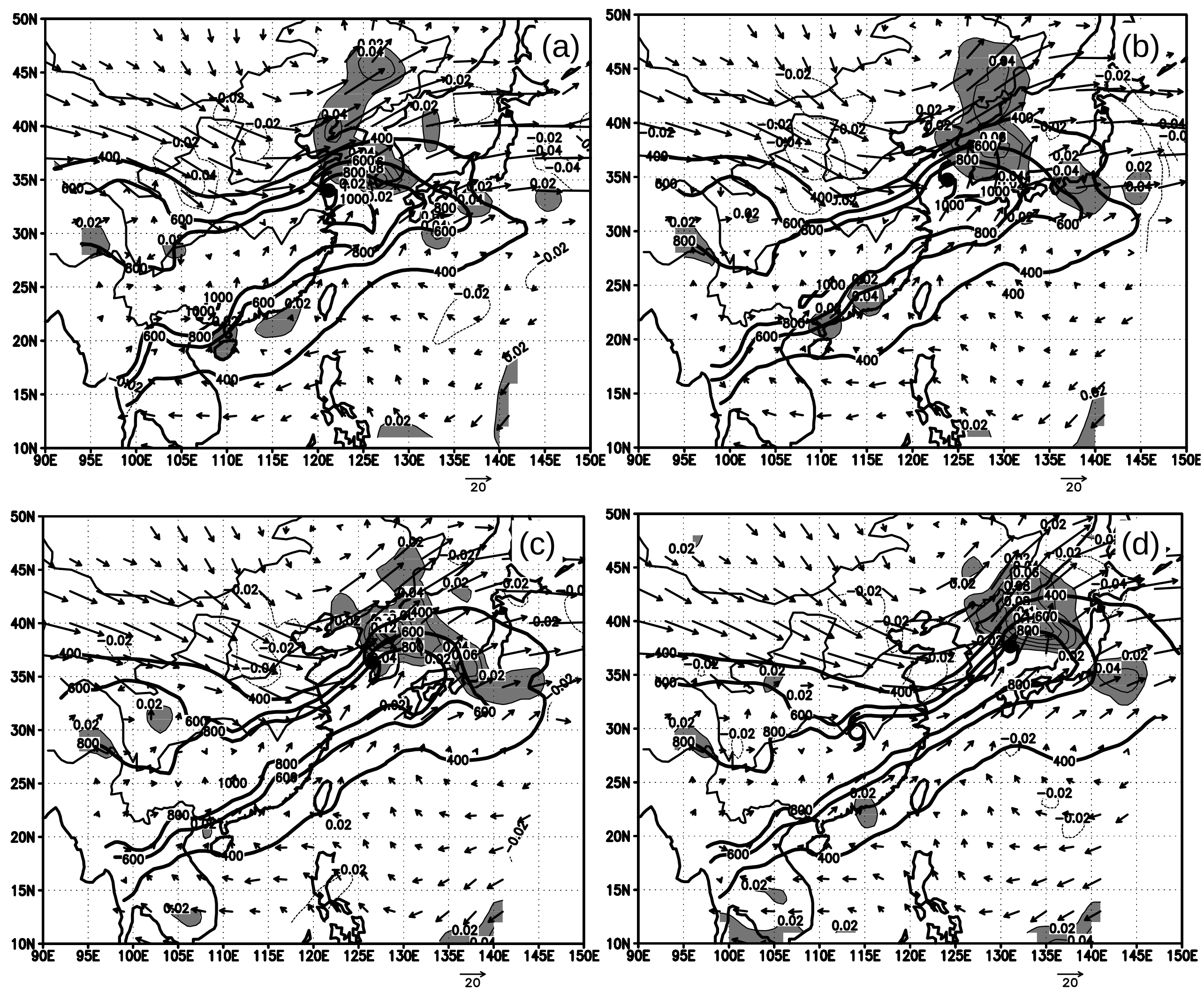


**Fig. 7.** Horizontal wind vectors and vertical velocity ($W$) on the 340 K moist isentropic surface. Solid lines are for isopiestics at an interval of 200 hPa, thin lines for vertical velocity at an interval of 2 cm s$^{-1}$, shaded areas denote the region with $W$ greater than 2 cm s$^{-1}$; solid and hollow cyclonic symbols denote the position of D1 and D2 respectively (from 0000 UTC 23 June to 1800 UTC 23 June 1999 at an interval of 6 h). (a) 0000 UTC 23 June; (b) 0600 UTC 23 June; (c) 1200 UTC 23 June; (d) 1800 UTC 23 June.

occur unless three conditions are satisfied: the presence of slantwise isentropic surfaces (or moist isentropic surfaces for moist air), up-sliding slantwise motions on isentropic surfaces, and $dC_{\mathrm{D}}/dt < 0$ (or $dC_{\mathrm{m}}/dt < 0$ for moist air). The first prerequisite can be seen to be satisfied near the Meiyu front from the analyses of Figs. 5–6; now the second prerequisite will be checked below.

Figure 7 shows the horizontal wind vectors and vertical velocity on the 340 K moist isentropic surface. The funnel-shaped pressure distribution is evident and the cyclones always move and develop near the northern slantwise moist isentropic surfaces. The cyclonic circulations (horizontal vectors) in front of D1 flow from higher pressures to lower ones and are superposed with positive W, that is, there are slantwise up-sliding motions immediately in front of D1 in the downwind direction. So the second prerequisite is satisfied. The mesoscale circulation of D1 interacts with the large-scale circulation and the isopiestics on the moist isentropic surface near D1 show some mesoscale distortions, which is favorable to the further development of the cyclone.

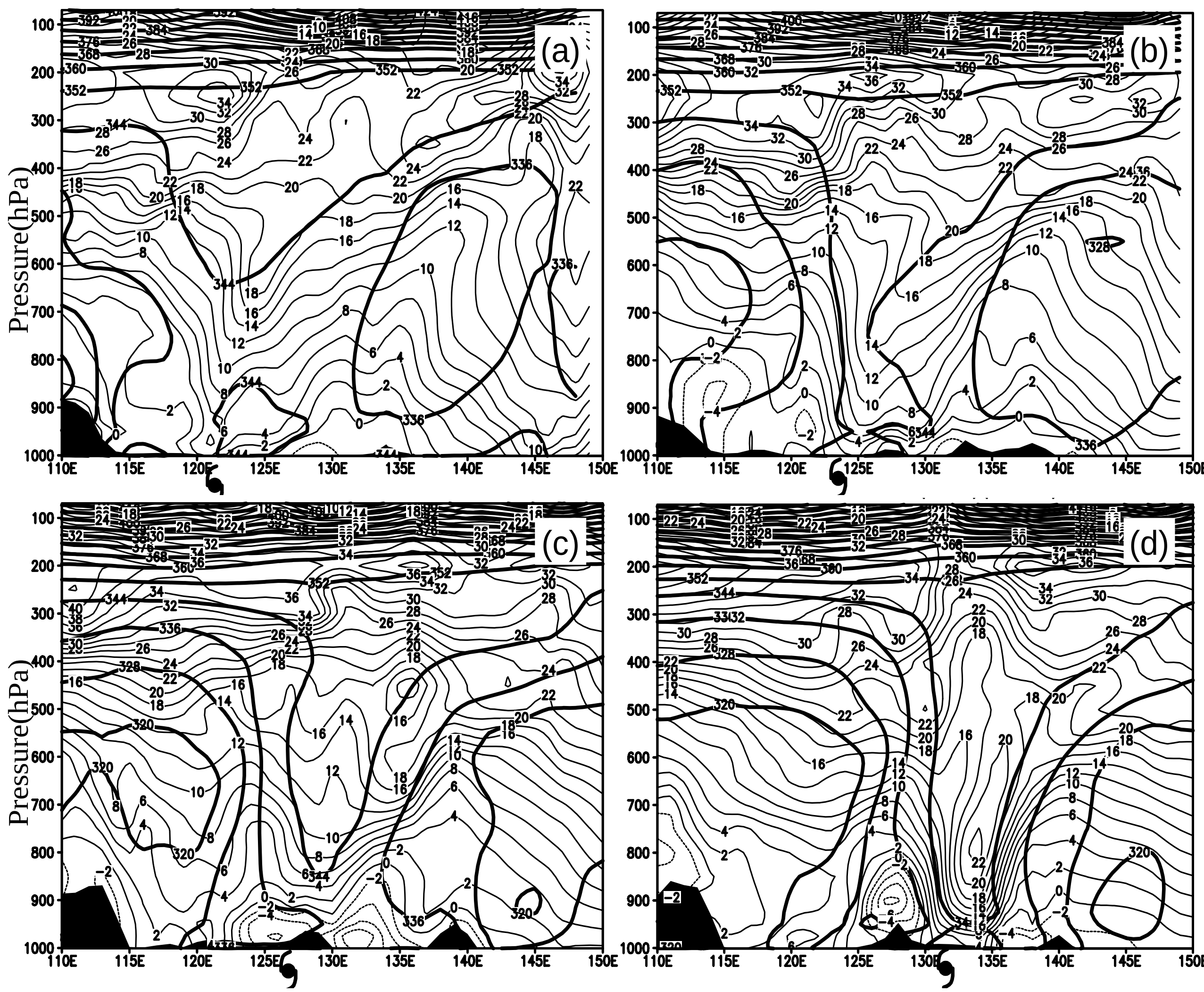


**Fig. 8.** Zonal cross-sections across the center of D1. Shaded areas are for topography, solid lines for moist isentropes, and thin lines for the $x$-component of velocity ($U$). The cyclonic symbol denotes the position of D1 (from 0000 UTC 23 June to 1800 UTC 23 June 1999 at an interval of 6 h). (a) 0000 UTC 23 June; (b) 0600 UTC 23 June; (c) 1200 UTC 23 June; (d) 1800 UTC 23 June.

From the analyses above, both of the first two prerequisites of USVD can be seen to be satisfied during the evolution of D1; but USVD will not occur unless the other condition, $dC_{\rm m}/dt < 0$, is also met. Figure 8 shows the zonal cross-sections across the center of D1. Apparent vertical shears of horizontal wind pointing vertically into the paper coexist with the evident slantwise up-sliding motions immediately in front of D1 in the downwind direction near the steep moist isentropic surface. From the studies above, this situation is equivalent to $C_{\rm m} < 0$, and since we have that when an air parcel starts to up-slide from the horizontal surfaces, $C_{\rm m} = 0$ (from Fig. 1, when isentropic surfaces are flat, $\theta_{\rm es} = 0$ and $C_{\rm m} = 0$), we get $dC_{\rm m}/dt < 0$ here. That is, USVD will occur immediately in front of D1 in the downwind direction and the cyclone will continue to move and develop in that direction. As we know, symmetric instability is a kind of mesoscale instability, which is important to the evolution of mesoscale weather systems. Regardless of the kind of instability, it is just a kind of status or property; there has to be some kind of start-up factors to arouse it to come into effect, and the slantwise up-sliding motions in USVD can be such a kind of start-up factor (detailed analyses will be done in a later paper).

## 7. Conclusions and discussion

In this paper, mass forcing is invoked to develop an MPV equation. Based on the theory of SVD, the theory of USVD is proposed to study the variation of vorticity caused by slantwise up-sliding motions along isentropic surfaces. From the definition of MPV and the MPV equation proposed above, a complete vorticity equation is put forward with mass forcing, which explicitly includes the effects of both internal forcings, such as variations of stability, baroclinicity, and vertical shear of horizontal wind, and external forcings, such as diabatic heat, friction, and mass forcing. When isentropic surfaces are flat, the complete vorticity equation is identical to the traditional counterpart. The physical interpretations of some of the items which are included in the complete vorticity equation but not in the traditional one are studied with a simplified model of the Changjiang-Huaihe Meiyu front; the results show that these extra terms represent the effects of frontogenesis, the variation of baroclinity, mass forcing, and so on. A torrential rain event in the Changjiang-Huaihe region is simulated and studied qualitatively based on the theory of USVD. The result tells us that the three conditions of the theory of USVD are easily met immediately in front of the mesoscale rainstorms, that is, USVD will appear immediately in front of the rainstorm. The theory of USVD is useful to the studies of the development and movement of these kinds of systems. As a kind of mesoscale instability, symmetric instability has a great impact on the evolution of mesoscale systems and the slantwise up-sliding motions of USVD may be a start-up factor of this kind of unstable energy.

In fact, it is common that most synoptic phenomena occur, develop, and move near steep isentropic surfaces, so to study these phenomena in the context of steep isentropic surfaces is helpful to our understanding of the physical mechanism of the phenomena. And SVD theory and the theory of USVD are just the vigorous tools to do that work. In future work, the theory of USVD and the corresponding complete vorticity equation will be used continuously to study the genesis, development, and movement of rainstorms by analyzing the output of high-resolution mesoscale models such as MM5 and ARPS.

***Acknowledgments.*** This work was supported by the Chinese Academy of Sciences Program of Well-Known Overseas Chinese Scholars under Dr. Samuel Shen and the Innovation Project of the Chinese Academy of Sciences under Grant No. KZCX3-SW-213 and by the National Natural Science foundation of China under Grant Nos. 40023001 and 40135020.

## REFERENCES

Bennetts, D. A., and B. J. Hoskins, 1979: Conditional symmetric instability-A possible explanation for frontal rainbands. *Quart. J. Roy. Meteor. Soc.*, **105**, 945–962.

Cui Xiaopeng, 2001: Study of slantwise vorticity development of subtropical cyclones. Ph. D. dissertation, Institute of Atmospheric Physics, Chinese Academy of Sciences, 146pp. (in Chinese)

Davis, C. A., and K. A. Emanuel, 1991: Potential vorticity diagnostics of cyclogenesis. *Mon. Wea. Rev.*, **119**, 1929–1953.

Ertel, H., 1942: *Ein Neuer Hydrodynamische Wirbdsatz.* Meteorology Zeitschr, Braunschweig, 277–281.

Gao Shouting, Tao Shiyan, and Ding Yihui, 1990: The generalized E-P flux of wave-meanflow interactions *Sciences in China* (Series B), **33**, 704–715.

Gao Shouting, Lei Ting and Zhou Yushu, 2002: Moist potential vorticity anomaly with heat and mass forcings in torrential rain systems. *Chin. Phys. Lett.*, **19**(6), 878–880.

Hoskins, B. J., M. E. McIntyre, and A. W. Robertson, 1985: On the use and significance of isentropic potential vorticity maps. *Quart. J. Roy. Meteor. Soc.*, **111**, 877–946.

Hoskins, B. J., and P. Berrisford, 1988: A potential vorticity perspective of the storm of 15–16 October 1987. *Weather*, **43**, 122–129.

Keyser, D., and R. Rotunno, 1990: On the formation of potential vorticity anomalies of upper-level jet front systems. *Mon. Wea. Rev.,* **118**, 1914–1921.

Montgomery, M. T., and B. F. Farrell, 1992: Polar low dynamics. *J. Atmos. Sci.,* **48**, 2484–2505.

Pedlosky, J., 1979: *Geophsical Fluid Dynamics.* Springer-Verlag, New York, 624pp.

Robinson, W. A., 1989: On the structure of potential vorticity in baroclinic instability. *Tellus,* **41A**, 275–284.

Schubert, W. H., and B. T. Alworth, 1987: Evolution of potential vorticity in tropical cyclones. *Quart. J. Roy. Meteor. Soc.*, **113**, 147–162.

Thorpe, A. J., 1990: Frontogenesis at the boundary between air-masses of different potential vorticity. *Quart. J. Roy. Meteor. Soc.*, **116**, 561–572.

Wu Guoxiong, and Liu Huanzhu, 1998: Vertical vorticity development owing to down-sliding at a slantwise isentropic surface. *Dynamics of Atmospheres and Oceans,* **27**, 715–743.

Wu Guoxiong, Cai Yaping, and Tang Xiaojing, 1995: Moist potential vorticity and slantwise vorticity development. *Acta Meteorologica Sinica,* **53,** 387–405. (in Chinese)

Wu Guoxiong, and Cai Yaping, 1997: Vertical wind shear and down-sliding slantwise vorticity development. *Scientia Atmospherica Sinica*, **21**, 273–281. (in Chinese)

Wu Guoxiong, and Liu Huanzhu, 1999: Complete form of vertical vorticity tendency equation and slantwise vorticity development. *Acta Meteorologica Sinica*, **57**, 1–13. (in Chinese)

Wu Guoxiong, 2001: Comparison between the complete-form vorticity equation and the traditional vorticity equation. *Acta Meteorologica Sinica*, **59**(4), 285–392. (in Chinese)

Zhang, D. -L., E. Radeva, and J. Gyakum, 1999: A family of frontal cyclones over the Western Atlantic Ocean.Part 1: A 60-h simulation. *Mon. Wea. Rev.*, **127**, 1725–1744.

Zhou Yushu, Gao Shouting, Samuel S. P. Shen, 2001: A diagnostic study of the structure and dynamical features of the Meiyu front system. *J. Meteor. Soc. Japan.* (submitted)